

Epitaxial growth of room-temperature ferrimagnetic semiconductor thin films based on the ilmenite-hematite solid solution

Hajime Hojo, Koji Fujita,^{a)} Katsuhisa Tanaka, and Kazuyuki Hirao

Department of Material Chemistry, Graduate School of Engineering, Kyoto University, Nishikyo-ku, Kyoto 615-8510, Japan

(Received 3 April 2006; accepted 29 June 2006; published online 24 August 2006)

Epitaxial thin films composed of $0.7\text{FeTiO}_3 \cdot 0.3\text{Fe}_2\text{O}_3$ solid solution have been prepared on $\alpha\text{-Al}_2\text{O}_3$ (0001) substrates by a pulsed laser deposition method, and their electrical and magnetic properties have been examined. A single phase of the ordered phase can be obtained under limited deposition conditions: oxygen partial pressure of 1.0×10^{-3} Pa and substrate temperature of 600–700 °C. The as-deposited film is semiconducting and ferrimagnetic below room temperature, while subsequent annealing in vacuum leads to the Curie temperature above room temperature. On the other hand, the thin films with the disordered phase appear to be antiferromagnetic and also insulating. © 2006 American Institute of Physics. [DOI: 10.1063/1.2337276]

Magnetic semiconductors with Curie temperature (T_C) beyond room temperature have attracted considerable attention since they are expected to be promising candidates for spin electronics applications. One approach to obtain magnetic semiconductors is to introduce the magnetic ions into nonmagnetic semiconductors, which is called diluted magnetic semiconductor (DMS). Since the discovery of room-temperature ferromagnetism in Co-doped TiO_2 ,¹ extensive studies have been carried out concerning DMS based on transition-metal-doped oxide semiconductors.² Another approach toward the development of magnetic oxide semiconductors is to explore semiconducting materials that are known to show ferromagnetism or ferrimagnetism above room temperature. Examples of such materials are solid solutions of ilmenite, FeTiO_3 , and hematite, $\alpha\text{-Fe}_2\text{O}_3$.

It is known that although both FeTiO_3 and $\alpha\text{-Fe}_2\text{O}_3$ are antiferromagnetic insulators,³ their solid solutions with intermediate compositions exhibit both semiconducting and ferrimagnetic properties.^{4,5} $\alpha\text{-Fe}_2\text{O}_3$ belongs to a family of corundum structure (space group: $R\bar{3}c$) and is composed of a distorted hcp of anions (O^{2-} ions). Fe ions occupy two-thirds of the available octahedral interstices, forming an alternate stack of Fe and O layers along the c axis. The crystal structure of FeTiO_3 is a derivative of corundum $\alpha\text{-Fe}_2\text{O}_3$; Fe layers stacked along the c axis in $\alpha\text{-Fe}_2\text{O}_3$ are alternatively replaced by Ti layers. Due to the replacement, the space group changes from $R\bar{3}c$ to $R\bar{3}$. Consequently, the solid solutions consisting of FeTiO_3 and $\alpha\text{-Fe}_2\text{O}_3$ undergo the order-disorder transition between $R\bar{3}$ and $R\bar{3}c$ symmetries. In the former, Ti ions exist only in alternate layers along the c axis as in FeTiO_3 . Since each cation layer is antiferromagnetically coupled with adjacent layers, strong ferrimagnetic properties are observed only when the crystal structure is the ordered phase. On the other hand, the disordered phase where cations are distributed at random, shows antiferromagnetic properties or rather weak magnetization.⁴

The uniqueness of this system lies in the fact that the conduction type can be controlled as either p or n type by

simply changing the composition. Furthermore, recent theoretical predictions suggested the possibility of spin-polarized carriers and high T_C in the solid solutions.⁶ In spite of such interesting electrical and magnetic properties, however, only a few studies have been reported on the solid solution or even on FeTiO_3 in the form of a thin film.^{7–10} Especially, it has never been demonstrated that semiconducting and ferrimagnetic thin films having T_C above room temperature could be obtained in the solid solutions. This is due to the difficulty in controlling the valence state of Fe ions as well as in stabilizing only the ordered phase during the film growth.⁹

In this letter, we present the preparation of thin films composed of the ordered phase of $0.7\text{FeTiO}_3 \cdot 0.3\text{Fe}_2\text{O}_3$ solid solutions using the pulsed laser deposition (PLD) technique. We also show that the as-deposited thin films are semiconducting and ferrimagnetic below room temperature, while the subsequent annealing treatment improves the magnetic properties; T_C is raised beyond room temperature.

Thin films with $0.7\text{FeTiO}_3 \cdot 0.3\text{Fe}_2\text{O}_3$ composition (in molar ratio) were grown on c -plane $\alpha\text{-Al}_2\text{O}_3$ (0001) substrates by a PLD method. The ceramic target used for PLD was prepared by the conventional solid-state reaction among powders of reagent-grade Fe_2O_3 and TiO_2 . A thin film was grown on the substrate by focusing a KrF excimer laser (wavelength: 248 nm) at a repetition frequency of 5 Hz with a fluence of 2–3 J/cm². To optimize the deposition condition, the substrate temperature (T_S) and the oxygen partial pressure (P_{O_2}) were varied from 600 to 800 °C and from 1.0×10^{-4} to 1.0×10^{-1} Pa, respectively. Some of the thin films were annealed under $P_{\text{O}_2} = 2.0 \times 10^{-4}$ Pa and $T = 700$ °C for 1 h in the vacuum chamber.

Rutherford backscattering spectroscopy was carried out using 2.0 MeV He^+ in order to determine the thickness and composition of the films. The analysis with the simulation program SIMNRA revealed that the film thickness was about 70 nm and that the fraction of Fe and Ti was typically 0.19:0.11, which means that $\text{FeTiO}_3:\text{Fe}_2\text{O}_3 = 0.73:0.27$. The crystal structure of the film was analyzed by x-ray diffraction (XRD) measurement with $\text{Cu } K\alpha$ radiation. Cross-sectional lattice images were obtained by means of a high-resolution transmission electron microscopy (HRTEM). Optical transmission spectra were measured using a spectrophotometer.

^{a)} Author to whom correspondence should be addressed; FAX: +81-75-383-2420; electronic mail: fujita@dipole7.kuic.kyoto-u.ac.jp

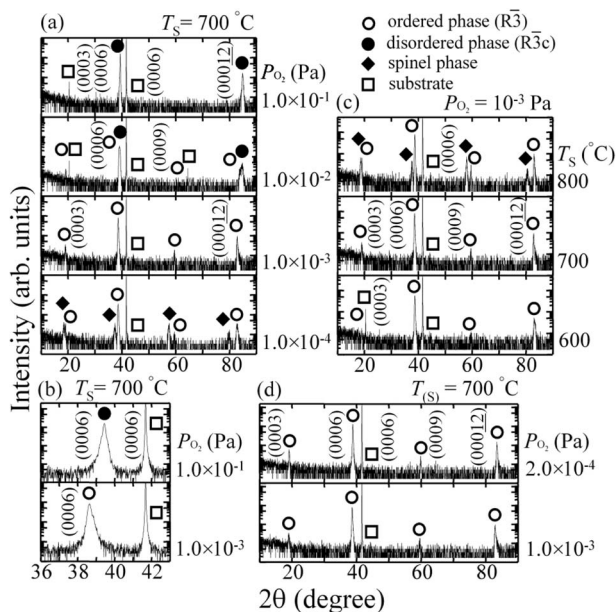


FIG. 1. (a) Variation of XRD pattern with P_{O_2} for the thin films grown under $T_S=700^\circ\text{C}$. (b) XRD patterns of the thin films grown at 1.0×10^{-3} and 1.0×10^{-1} Pa in the expanded scale. (c) Variation of XRD pattern with substrate temperature for the thin films grown under $P_{O_2}=1.0\times 10^{-3}$ Pa. (d) XRD patterns of the ordered-phase solid solution thin films before and after annealing at $T=700^\circ\text{C}$ and $P_{O_2}=2.0\times 10^{-4}$ Pa. Open circles, closed circles, and closed diamonds denote the diffraction peaks due to the ordered phase, the disordered phase, and the spinel phase, respectively.

The measurements of magnetization were carried out using a superconducting quantum interference device magnetometer. The electric resistivity was measured by the van der Pauw method. The Seebeck coefficient was determined at room temperature to identify the major conduction type.

Figure 1(a) shows XRD patterns for $0.7\text{FeTiO}_3\cdot 0.3\text{Fe}_2\text{O}_3$ films grown at $T_S=700^\circ\text{C}$ under various P_{O_2} . One can see that the thin film grown under $P_{O_2}=1.0\times 10^{-3}$ Pa is composed of the single phase of (0001)-oriented $\text{FeTiO}_3\text{-Fe}_2\text{O}_3$ solid solution with the ordered phase ($R\bar{3}$ symmetry). When P_{O_2} is decreased to 1.0×10^{-4} Pa, the crystalline phase ascribed to a spinel-type structure is observed as an impurity phase. On the contrary, as P_{O_2} is increased from 1.0×10^{-2} Pa, the disordered phase ($R\bar{3}c$ symmetry) starts to appear: one can identify the crystal symmetry of the film, since only (0006n) peaks are observed in the disordered phase with the $R\bar{3}c$ symmetry due to a systematic absence. The thin film grown at P_{O_2} as high as 1.0×10^{-1} Pa contains the disordered phase only. Expanded XRD patterns for the thin films grown at 1.0×10^{-3} and 1.0×10^{-1} Pa [Fig. 1(b)] reveal that the positions of diffraction peaks for the disordered phase are observed at higher diffraction angle sides, indicating that the lattice constant is reduced along the c axis. This is presumably due to the oxidation of Fe^{2+} to Fe^{3+} during the deposition at higher P_{O_2} , which suppresses the growth of films with the ordered phase, and also due to the change in crystal symmetry from $R\bar{3}$ to $R\bar{3}c$.⁸ We have also examined the effect of the T_S on the crystalline phase of the deposited films. The results for the films grown under $P_{O_2}=1.0\times 10^{-3}$ Pa are shown in Fig. 1(c). The thin films grown at $T_S=600$ and 700°C are single phases of the ordered phase, whereas the thin film grown at

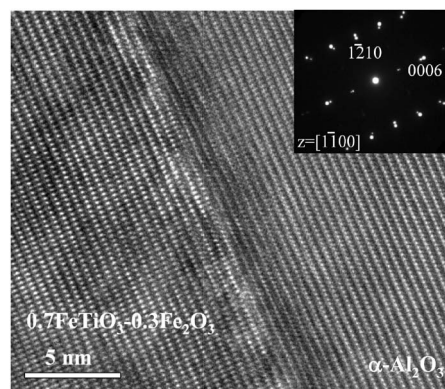


FIG. 2. Cross-sectional HRTEM image and SAED pattern of the ordered-phase film deposited on $\alpha\text{-Al}_2\text{O}_3$. The direction of the incident electron is parallel to the $[1\bar{1}00]$ direction of $\alpha\text{-Al}_2\text{O}_3$.

$T_S=800^\circ\text{C}$ contains the crystalline phase with the spinel-type structure in addition to the ordered phase. From the results of Figs. 1(a) and 1(c), it is found that the crystalline phase such as Fe_2TiO_4 (ulvöspinel-type structure) also tends to be stabilized under lower P_{O_2} and higher T_S , both deposition conditions of which prompt the production of Fe^{2+} .

In Fig. 1(d) is compared the XRD pattern for the as-deposited thin film grown under $P_{O_2}=1.0\times 10^{-3}$ Pa and $T_S=700^\circ\text{C}$ with that for the thin film postannealed at 700°C in vacuum ($P_{O_2}=2.0\times 10^{-4}$ Pa). No secondary impurity phase is detected in the annealed thin film. By the annealing treatment, the positions of diffraction peaks shift to higher angles, indicating the reduction of the lattice constant along the c axis. The reduction of lattice constant is not ascribed to the oxidation of Fe^{2+} to Fe^{3+} mentioned above, since the annealing treatment under lower P_{O_2} favors the production of Fe^{2+} , which would increase the lattice constant. Instead, we believe that the improvement of the crystallinity is more significantly responsible for the decrease in lattice constant.

Figure 2 shows a cross-sectional HRTEM image of $0.7\text{FeTiO}_3\cdot 0.3\text{Fe}_2\text{O}_3$ solid solution thin film with the ordered phase on $\alpha\text{-Al}_2\text{O}_3$ and selected area electron diffraction (SAED) pattern. The HRTEM image exhibits highly epitaxial nature of the film with no impurity phases. The SAED pattern reveals the in-plane and out-of-plane epitaxial growths of the film. The epitaxial relationship is as follows: solid solution film (0001) $[1\bar{1}00]$ // Al_2O_3 (0001) $[1\bar{1}00]$. The (01 $\bar{1}2$) pole figure of the thin film (not shown) also demonstrated this epitaxial relationship.

Optical transmission spectra measured at room temperature are shown in Fig. 3. The measurements were performed not only for the annealed film with the ordered phase but also for the film with the disordered phase. In the inset, $(\alpha h\nu)^2$ is plotted against $h\nu$ to evaluate the optical band gap, where α and $h\nu$ denote the absorption coefficient and photon energy, respectively. The optical band gap, obtained from the intercept of the dotted extrapolated line and abscissa, is estimated to be ~ 3.3 eV for the ordered phase and ~ 2.7 eV for the disordered phase.

Temperature dependence of electric resistivity (ρ) is shown in Fig. 4 for as-deposited and annealed films with the ordered phase. Room-temperature ρ for the film with the disordered phase is also shown for comparison. Both of the ordered-phase films show thermal-activation-type tempera-

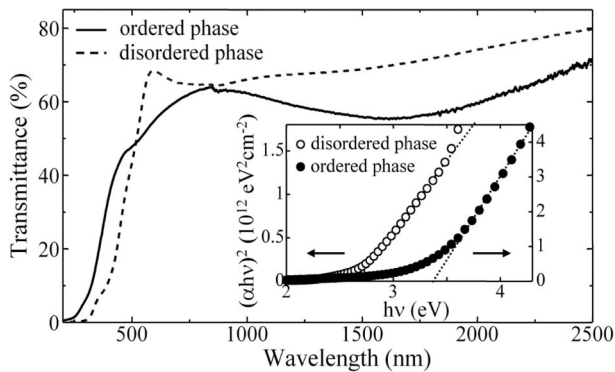


FIG. 3. Optical transmission spectrum for the annealed film with the ordered phase (solid curve) and the film with the disordered phase (dashed curve). The inset shows the plot of $(\alpha hv)^2$ vs $h\nu$ for estimation of direct allowed band gap (closed circles: ordered phase; open circles: disordered phase).

ture dependence over a range of 70–350 K. The activation energy estimated using the formula $\rho = \rho_0 \exp(E/kT)$ is about 0.07 eV for both of the films. This value is comparable to those in bulk and thin film samples as reported previously.^{5,7} On the other hand, ρ for the disordered-phase film is three orders of magnitude higher than that for the film with the ordered phase. High ρ is caused by a considerably small amount of Fe^{2+} ions in the disordered-phase thin film prepared under high P_{O_2} , because Fe^{3+} and Fe^{2+} pairs contribute to the electrical conduction in this system.⁵ The Seebeck coefficient of the annealed film with the ordered phase was found to be almost zero; that is, within a measurable limit of our apparatus, contributions of electrons and holes to conduction are comparable to each other. This result is reasonable because the present composition falls on the border between p and n types, and the Seebeck coefficient is expected to be small near this composition.⁵

Figure 5 shows magnetization (M) as a function of an external magnetic field (H) at room temperature for the as-deposited and annealed films with the ordered phase and the film with the disordered phase. Large M and a well-defined hysteresis loop are observed only for the annealed film with the ordered phase. Dependence of M on temperature (T) is displayed in the inset of Fig. 5. The measurements were performed under a field-cooled condition, while H of 8500 Oe was applied parallel to the film surface. For the as-deposited and annealed films with the ordered phase, M increases almost linearly with a decrease in temperature below a critical

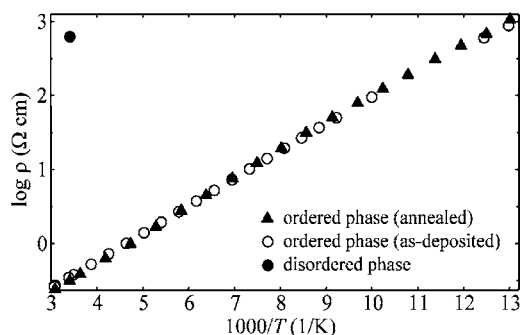


FIG. 4. Temperature dependence of ρ for films with the ordered phase (open circles: as-deposited; closed triangles: annealed). Room-temperature ρ for the film with the disordered phase is also shown (a closed circle).

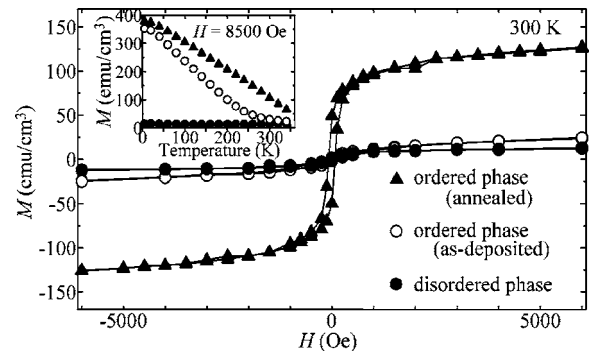


FIG. 5. Room-temperature M - H curves for the thin films with the ordered phase (open circles: as-deposited; closed triangles: annealed) and that with disordered phase (closed circles). The inset shows temperature dependence of M measured at $H=8500$ Oe under a field-cooled condition.

temperature. The T_C is below room temperature for the as-deposited film, while the annealing raises the T_C above room temperature. A similar M - T curve was observed for the bulk samples of FeTiO_3 - Fe_2O_3 solid solution and ascribed to the R -type ferrimagnetism.⁴ However, we observed that zero-field-cooled M deviates from field-cooled M at a certain temperature when a low H such as 300 Oe is applied, which is indicative of finite-range ferrimagnetic ordering. This phenomenon may arise since the distribution of Fe and Ti ions in the film with the ordered phase is slightly different from the ideal arrangement as Ishikawa¹¹ described previously, by which long-range ferrimagnetic ordering can be developed. For the film with the disordered phase, on the other hand, M is very small and exhibits almost no temperature dependence, suggesting that the film is antiferromagnetic in this temperature range.

In conclusion, we have grown $0.7\text{FeTiO}_3 \cdot 0.3\text{Fe}_2\text{O}_3$ solid solution thin films on $\alpha\text{-Al}_2\text{O}_3$ (0001) substrates using the PLD method to examine their electrical and magnetic properties. The growth of solid solution thin film consisting of the ordered phase ($R\bar{3}$ symmetry) is reproducibly achieved by tuning the oxygen partial pressure and substrate temperature during the deposition. We also found that the ordered-phase films annealed at 700 °C in vacuum are ferrimagnetic with T_C above room temperature.

One of the authors (K.F.) acknowledges financial support from Yazaki Foundation.

¹Y. Matsumoto, M. Murakami, T. Shono, T. Hasegawa, T. Fukumura, M. Kawasaki, P. Ahmet, T. Chikyow, S. Koshihara, and H. Koinuma, *Science* **291**, 854 (2001).

²T. Fukumura, H. Toyosaki, and Y. Yamada, *Semicond. Sci. Technol.* **20**, S103 (2005).

³To be exact, $\alpha\text{-Fe}_2\text{O}_3$ shows canted spin magnetism. L. Néel, *Ann. Phys. (Paris)* **4**, 249 (1949).

⁴Y. Ishikawa and S. Akimoto, *J. Phys. Soc. Jpn.* **12**, 1083 (1957).

⁵Y. Ishikawa, *J. Phys. Soc. Jpn.* **13**, 37 (1958).

⁶W. H. Butler, A. Bandyopadhyay, and R. Srinivasan, *J. Appl. Phys.* **93**, 7882 (2003).

⁷F. Thou, S. Kotru, and R. K. Pandey, *Thin Solid Films* **408**, 33 (2002).

⁸T. Fujii, M. Kayano, Y. Takada, M. Nakanishi, and J. Takada, *J. Magn. Mater.* **272-276**, 2010 (2004).

⁹T. Fujii, M. Kayano, Y. Takada, M. Nakanishi, and J. Takada, *Solid State Ionics* **172**, 289 (2004).

¹⁰Z. Dai, P. Zhu, S. Yamamoto, A. Miyashita, K. Narumi, and H. Naramoto, *Thin Solid Films* **339**, 114 (1999).

¹¹Y. Ishikawa, *J. Phys. Soc. Jpn.* **17**, 1835 (1962).